Biomaterials Science

PAPER

View Article Online
View Journal | View Issue

Cite this: *Biomater. Sci.*, 2019, **7**, 1607

A polyethylenimine-based diazeniumdiolate nitric oxide donor accelerates wound healing

Yan Zhang,†[a] Keyu Tang,†[b] Bin Chen,[b] Su Zhou,[c] Nan Li,[b] Chuwei Liu,[d] Jianyong Yang,[b,c] Run Lin, *[b,c] Tao Zhang *[a] and Weiling He*[d]

Nitric oxide (NO) plays a pivotal role in the cutaneous healing process and a topical supplement of NO is beneficial for wound repair. In this work, a novel polyethylenimine (PEI) based diazeniumdiolate nitric oxide donor was prepared. The obtained polymer (PEI-PO-NONOate) was characterized by Fourier transform infrared (FTIR) spectroscopy, UV-vis absorption spectra, and nuclear magnetic resonance (NMR). The PEI-PO-NONOate polymer was stable under anhydrous conditions at different temperatures. A total of 0.57 μmol gaseous NO was released from 1.0 mg of the PEI-PO-NONOate polymer in PBS of pH 7.4 and it presented a proton-driven release pattern. Furthermore, the PEI-PO-NONOate polymer exhibited a controlled release profile sustained for over 30 hours within the polyethylene glycol (PEG) mixture system. Cytotoxicity evaluation was performed on L929 cells. Full-thickness excisional cutaneous wound models of mice were prepared and the PEI-PO-NONOate polymer was applied to investigate its effects on wound healing. The results revealed that the PEI-PO-NONOates exhibited good biocompatibility. It was also found that the PEI-PO-NONOate polymer promoted cutaneous wound healing and closure with enhanced granulation tissue formation, collagen deposition, and angiogenesis, as compared to the control. In summary, a novel nitric oxide releasing polymer with high loading efficiency and a controlled release profile was developed which presented the potential for application in the acceleration of cutaneous wound healing.

Received 22nd November 2018,
Accepted 16th January 2019

DOI: 10.1039/c8bm01519h

rsc.li/biomaterials-science

1. Introduction

Impaired cutaneous wound repair remains a great clinical challenge which not only gives rise to tremendous pathological issues such as persistent symptoms, infection, and scar healing, but also brings an estimated annual economic burden at a magnitude of billions of dollars, as well as psychological stress.[1,2] However, optimum treatment options are still lacking, demanding the development of novel strategies to accelerate wound healing.

As significant progress has been achieved in understanding the underlying mechanisms of wound repair recently, a variety of cytokines, chemokines and growth factors involved were identified. Among them, nitric oxide (NO) is one of the most important factors in the regulation of the three cascaded and overlapping phases, inflammation, proliferation and remodeling, of the wound healing process, exerting biological effects including antibacterial properties, enhancing collagen synthesis and deposition, promoting angiogenesis, *etc.*[3–5] The importance of NO in wound healing has been proved at different levels and from different perspectives.[3] For instance, the levels of nitric oxide metabolites correlate with the healing trajectory,[6] indicating the tendency of recovery or exacerbation. The topical application of exogenous gaseous NO or the nitric oxide synthase (NOS) stimulator,[7] the transfer of the NOS gene,[8,9] and the systemic supply of the NOS substrate[10] are all capable of elevating the local NO concentration, and consequently, promoting wound recovery. On the other hand, a blockade or knockout of NOS, or the clearance of NO by a scavenger impairs wound healing.[11,12] Furthermore, the inhibition of arginase, the enzyme which hydrolyses arginine substantially faster than NOS and consequently depletes the substrate for NO synthesis, accelerates wound healing.[13,14] The beneficial effects of nitric oxide make the modulation of the NO signal pathway an attractive approach for the promotion of wound healing.

Among the aforementioned strategies, the topical application of NO-releasing or NO-generating biomaterials represents the most convenient and effective approach. These substances consist of numerous sorts of vehicles for local NO delivery such as nanoparticles, hydrogels, polymers, and so

[a]*College of Engineering and Applied Sciences, Nanjing University, Nanjing, 210093, China. E-mail: ztnj@nju.edu.cn*
[b]*Department of Radiology, First Affiliated Hospital, Sun Yat-sen University, Guangzhou, Guangdong 510080, China. E-mail: hewling@mail.sysu.edu.cn, linrun5@mail.sysu.edu.cn*
[c]*School of Biomedical Engineering, Xinhua College of Sun Yat-sen University, Guangzhou, Guangdong, 510520, China*
[d]*Department of Gastrointestinal Surgery, First Affiliated Hospital, Sun Yat-sen University, Guangzhou, Guangdong 510080, China*
†These authors contributed equally.

forth.[15,16] Despite the fact that significant progress has been achieved, challenges including burst release behavior, inferior biocompatibility, and low loading efficiency are yet to be overcome.[17] Polymer-based NO donors hold great promise because of their versatility for modification, easy processability, tailored properties, high payload, *etc*.[17,18] Recently, diazeniumdiolates (NONOates) entered the mainstay of the development of NO donors, taking advantage of their high loading efficiency and optimal NO release kinetics to achieve predictable and controlled NO delivery.[17]

In this work, a novel diazeniumdiolate nitric oxide donor was prepared using propylene oxide (PO) modified polyethylenimine (PEI) and gaseous NO. The obtained polymer (PEI-PO-NONOate) was characterized by Fourier transform infrared (FTIR) spectroscopy, UV-vis absorption spectra, and nuclear magnetic resonance (NMR). The storage stability of PEI-PO-NONOates was studied under anhydrous conditions at different temperatures (−18 °C, 4 °C, and 35 °C), and the release profiles were investigated in PBS of different pH values and within the polyethylene glycol (PEG) mixture system. The cytotoxicity assay was performed on mouse fibroblast cells (L929). The effect of PEI-PO-NONOates on wound healing was investigated *in vivo* using a mouse full-thickness cutaneous wound model. Wound areas and the wound closure of the NO treatment group and the control group were determined and compared. Histological analysis including hematoxylin–eosin (HE), Masson trichrome and Sirius Red staining, as well as immunohistochemistry and immunofluorescence studies of CD31 and VEGF, were performed to investigate and elucidate the underlying mechanisms.

2. Materials and methods

2.1. Materials

Branched polyethylenimine (PEI, MW 1800, 99%), propylene oxide (PO, ≥99%) and sodium methoxide (≥97%) were purchased from Aladdin Industrial Corporation (Shanghai, China). Ethanol, methanol and tetrahydrofuran (THF, AR) were obtained from Nanjing Chemical Reagent Co., Ltd (Nanjing, China). The nitric oxide assay kit (Griess reagent) was obtained from Beyotime Institute of Biotechnology (Shanghai, China). NO gas (≥99.9%) was obtained from Nanjing Tianze Gas Co., Ltd (Nanjing, China). Mouse fibroblast cells (L929) were purchased from the American Type Culture Collection (ATCC, Manassas, VA, USA). Roswell Park Memorial Institute 1640 (RPMI 1640, containing L-glutamine) was purchased from Gibco (Thermo Fisher Scientific, Waltham, MA, USA). Fetal bovine serum (FBS) was purchased from Zhejiang Tianhang Biological Technology Stock Co., Ltd (Hangzhou, China), and was heated for 30 min at 56 °C for sterilization, and then cryopreserved at −20 °C for later use. The cell counting kit-8 (CCK-8), polyethylene glycol (PEG, MW 400) and pentobarbital sodium (>99%) were purchased from Dojindo China Co., Ltd (Shanghai, China), Sigma-Aldrich (Saint Louis, MO, USA) and MSD China (Shanghai, China), respectively. The anti-VEGF antibody (rabbit polyclonal IgG, 1 : 200 dilution, Cat. no. GB11034), anti-CD31 antibody (rabbit polyclonal IgG, 1 : 400 dilution, Cat. no. GB11063), Cy3 conjugated goat anti-rabbit IgG (heavy + light chain, 1 : 300 dilution, Cat. no. GB21303), Tris–EDTA buffer antigen retrieval solution (pH 9.0, Cat. no. G1203), and 4′,6-diamidino-2-phenylindole (DAPI, Cat. no. G1012) were purchased from Servicebio (Wuhan, China).

2.2. Preparation of PEI-PO-NONOates

The synthetic route of PEI-PO-NONOates is shown in Fig. 1. Polyethylenimine (PEI) was dissolved in absolute ethanol, and propylene oxide (PO) with equal moles of the primary amine on PEI molecules was added to the solution in an ice-water bath while stirring. After reacting for 2 days, the solution was dried under vacuum for another 2 days to obtain the PEI-PO sample. Then the sample was dissolved in an absolute methanol/tetrahydrofuran mixture (volume ratio 1 : 1). Sodium methoxide/methanol solution (33 mg mL^{-1}) was added and the mixture was charged in a 50 mL micro-autoclave (Senlong Company, Beijing, China) and deoxidized using pure nitrogen. Subsequently, the micro-autoclave was filled with NO gas until the pressure reached 0.55 MPa and was maintained for 3 days.[19,20] After that, the crude product was washed with cold diethyl ether and methanol repeatedly at least 3 times. Finally,

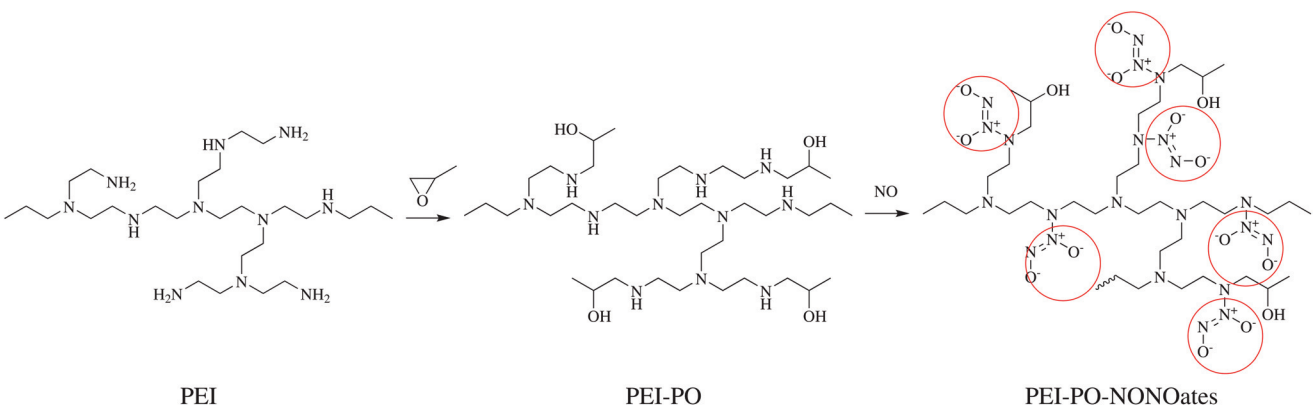

Fig. 1 Synthetic route of PEI-PO-NONOates.

the PEI-PO-NONOate polymer was obtained and cryopreserved at −18 °C.

2.3. Characterization

Fourier transform infrared (FTIR) spectroscopy was used to study the changes in the structures of PEI, PEI-PO and PEI-PO-NONOates using a PE GX Fourier transform infrared spectrometer (PerkinElmer, Boston, MA, USA). The UV-vis absorption peak strength of [N(O–)N═O]– at a wavelength of 250 nm was measured by immersing PEI-PO-NONOates in PBS (0.15 mg mL^{-1}) using a UV-1800PC spectrophotometer (MAPADA, Shanghai, China). Subsequently, the chemical structures of PEI, PEI-PO and PEI-PO-NONOates were further determined by nuclear magnetic resonance (^{1}H-NMR and ^{13}C-NMR) in D_2O using a 500 MHz NMR spectrometer (Bruker ARX 500, Germany).

2.4. NO releasing profiles and stability

The NO releasing profiles of PEI-PO-NONOates were investigated under various conditions for different evaluations. For the NO releasing evaluation in PBS, the PEI-PO-NONOate samples were incubated in vials with PBS of pH 6.0 and 7.4, respectively, at a temperature of 35 °C. At scheduled timepoints, 50 μL solution was collected from each vial for testing while an equal volume of fresh PBS was added. The Griess reagent I and II were added to the samples and then the samples were measured at 540 nm using a microplate spectrofluorometer RT-6000 (Rayto, Shenzhen, China). The amounts of released NO were calculated by the optical density (OD) value according to the standard curve of the Griess reagent determined in advance. Furthermore, the NO releasing evaluation in the PEG mixture was investigated by determining the residual NO in the PEI-PO-NONOate samples after being mixed with PEG and storing at room temperature (25 °C) in open vials, using the Griess reagent and the same method described earlier. The amounts of released NO were calculated using the following equation (eqn (1))

$$NO_{released} = NO_{original} - NO_{residual} \quad (1)$$

where $NO_{released}$, $NO_{original}$ and $NO_{residual}$ are the released, original and residual amounts of NO, respectively.

In order to evaluate the stability of PEI-PO-NONOates under specified storage conditions, certain amounts of samples were sealed in polypropylene containers and stored in an oven at 35 °C, in a refrigerating chamber at 4 °C and in a freezing chamber at −18 °C, respectively. At scheduled timepoints, the samples were dissolved in PBS. The amounts of residual NO were measured by the Griess reagent method.

2.5. *In vitro* cell cytotoxicity assay

To evaluate the biocompatibility of the PEI-PO-NONOates, L929 cells were cultured in RPMI-1640 medium, supplemented with 15% FBS, and 1% penicillin–streptomycin at 37 °C under a humidified atmosphere of 95% air and 5% CO_2. 5×10^3 cells were seeded into each well of a 96-well plate and grown for 24 h before the experiments were performed. The PEI-PO-NONOates, PEI-PO, and PEI were dissolved in saline, respectively, and the solutions were filtered and sterilized with a 0.22-micron filter. Then the PEI-PO-NONOates, PEI-PO, and PEI solutions were added into the culture media at different concentrations (5–100 μg mL^{-1}), respectively. The cells were cultured for 24 hours followed by cell viability analysis (n = 6) using the CCK-8 kit. The cell viabilities were calculated using the following equation (eqn (2)):

$$\text{Cell viability} = (OD_{sample} - OD_{blank})/(OD_{control} - OD_{blank}) \times 100\% \quad (2)$$

where OD is the optical density value recorded using a microplate spectrofluorometer RT-6000 (Rayto, Shenzhen, China) and the subscripts (sample, control and blank) represent the sample groups, control groups and the blank groups, respectively.

2.6. *In vivo* wound healing assay

All animal study protocols were reviewed and approved by the Animal Care Committee of Sun Yat-sen University, and the experiments were performed in accordance with the National Institutes of Health's guidelines for the use of experimental animals. Male BALB/c mice weighing 20 to 30 g were purchased from the Laboratory Animal Center of Sun Yat-Sen University. Six mice were anesthetized by intraperitoneal injection of pentobarbital sodium (50 mg kg^{-1}). The dorsal portions of the mice were shaved and then the skin was sterilized with iodine followed by a rinse with 70% (vol/vol) ethanol. After that, the mice were placed on sterile sheets and the dorsal portion of the skin was pulled from the midline with tweezers. Full-thickness cutaneous wounds were created symmetrically on both sides using a Harris Uni-Core Punch (a 5.0 mm coring device, GE Healthcare, Piscataway, NJ, USA). Self-adhesive film dressings (SOFIT® 3000, Beijing, China) were applied for the wounds and the mice were then placed on a heating blanket until complete recovery.

Given the strong inhibition effect of NO upon coagulation,[21] the treatment was started one day after wounding, allowing the formation of blood clots. The PEI-PO-NONOate polymer was mixed with PEG at a concentration of 5 mg mL^{-1} right before each treatment. The lesions on one side were treated with the PEI-PO-NONOate/PEG mixture whereas the wounds on the other side were subjected to PEG alone as the control.

The PEI-PO-NONOate/PEG mixture or PEG, with a volume of approximately 20 μL, was topically applied to the wounds on days 1, 4, 7, and 10 post wounding. Sterile silicone rings with an internal diameter of 6 mm were glued around the wounds to minimize the contraction throughout healing and each mouse received a self-adhesive film dressing. The wounds were rinsed with sterile saline before each treatment and the silicone rings and the film dressings were replaced with new ones after treatment. The mice were then placed on a heating blanket after treatment until complete recovery. Scaled digital images of the wounds were captured (Nikon, D3500) at an identical height on days 1, 7, 11 and 14 after wounding. The wound areas were quantified from three measurements of

each image by two investigators who were blind to the treatments using ImageJ software (National Institutes of Health, Bethesda, MD, USA) and the percentage of wound closure was calculated using the following equation (eqn (3)):

$$A = \left(\frac{A_{pre} - A_{post}}{A_{pre}}\right) \times 100\% \quad (3)$$

where A is the percentage of wound closure, A_{pre} is the wound area 1 day after wounding, and A_{post} is the wound area on days 7, 11 and 14 after wounding.

2.7. Histology and immunohistochemistry experiments

Three mice were sacrificed by cervical dislocation 7 days post wounding. The wounds and the adjacent normal skin were collected and fixed with 4% paraformaldehyde for histological examinations. Then the samples were subjected to hematoxylin–eosin (HE) staining to study the states of wound healing. Masson trichrome and Sirius Red staining were carried out to determine the synthesis and deposition of collagen. Meanwhile, immunohistochemical and immunofluorescence examinations were performed to investigate angiogenesis as determined by the expressions of CD31 and VEGF. The stained samples were surveyed and the images were obtained using a Nikon Eclipse TI-SR microscope with a DS-U3 image-capturing system (Nikon, Japan), or an Olympus BX51WI microscope with an UIS2 optical system (Olympus, Japan).

2.8. Statistical analysis

The results were calculated by averaging the data from multiple measurements and presented as mean ± standard deviations. A one-tailed unpaired t-test was used to analyze the statistical significance for a comparison of the results and the level of significance was set at $p < 0.05$.

3. Results and discussion

3.1. Characterization

The structural transformations of PEI, PEI-PO and PEI-PO-NONOates were characterized by FTIR spectroscopy, UV-vis spectra, and NMR (Fig. 2). In the FTIR spectrum of PEI as shown in Fig. 2A, the peak at 3276 cm^{-1} and the strong absorbance at 1605 cm^{-1} represented the typical structure of the primary amine ($-NH_2$) while the wide absorbance from 3300 to

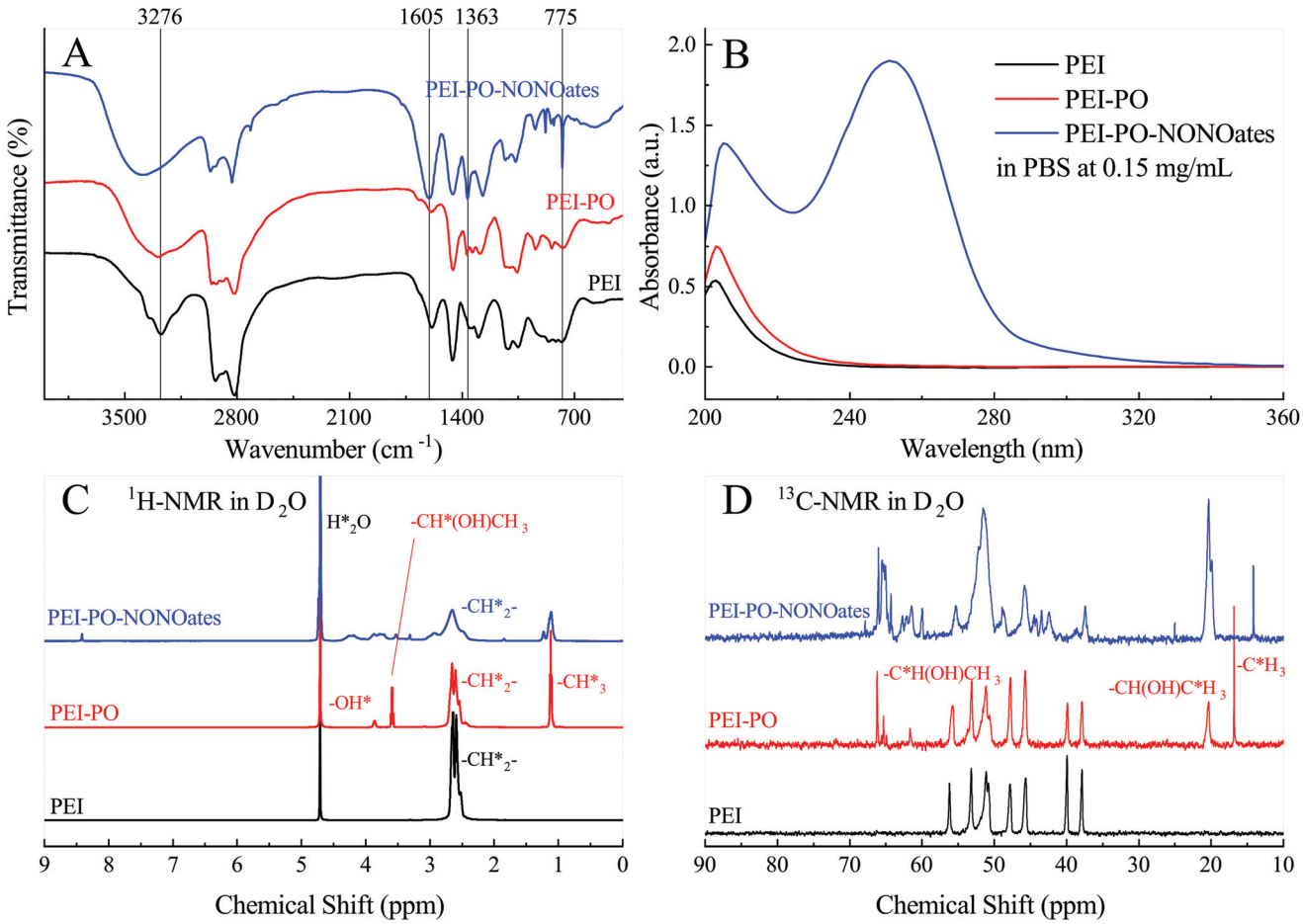

Fig. 2 Chemical characterization of PEI-PO-NONOates. (A) FTIR spectra, (B) UV-vis curves, (C) ^{1}H-NMR spectra and (D) ^{13}C-NMR spectra of PEI, PEI-PO and PEI-PO-NONOates in D_2O.

3400 cm^{-1} should be assigned to the secondary amine (–NH–) group. The other peaks were all identical to the branched PEI with a low molecular weight. After the addition reaction with PO, the curve of PEI-PO showed the typical aliphatic alcohol structure, exhibiting the absorbance from 3200 to 3600 cm^{-1}. Furthermore, on the curve of PEI-PO-NONOates, the peak at 1363 cm^{-1} should be assigned to the nitrate structure. Along with the peaks at 1605 and 775 cm^{-1}, these three peaks showed the typical FTIR spectrum of the *N*-diazeniumdiolate structure which proved the successful synthesis of PEI-PO-NONOates.[22]

The UV-vis spectra of PEI, PEI-PO and PEI-PO-NONOates are shown in Fig. 2B. The absorbance at a wavelength of 250 nm was attributed to the specific peak of the [N(O–)N=O]– group in PEI-PO-NONOates, which also verified the success of the synthesis. Fig. 2C shows the ^{1}H-NMR spectra in D_2O of the samples. In the spectrum of PEI, the resonance peak at 4.7 ppm represented the protons from the residual H_2O while the multiple peaks at 2.7 ppm represented the hydrogen atoms in the methylene groups (–CH^*_2–). The addition of PO introduced the CH_3 groups which presented the resonance peak at 1.1 ppm (–CH^*_3) while the –CH^*(OH)CH_3 groups showed the resonance peak at 3.6 ppm, and the OH groups showed the resonance peak at 3.8 ppm. Further reactions with NO did not introduce any new hydrogen-containing group but the changes in the chemical environment widened and shifted the resonance peaks of the existing groups which appeared at 1.8, 3.3, 4.2 and 8.4 ppm. The ^{13}C-NMR spectra of the samples are shown in Fig. 2D. As compared to the ^{13}C-NMR spectrum of PEI, the new peaks at 16.8 ppm and 20.4 ppm on the curve of PEI-PO reflected the existence of carbon atoms in the CH_3 groups, and the difference in the chemical shifts was caused by the different sites on the branched PEI. The other two new peaks at 65.3 ppm and 66.2 ppm were due to the resonance of the carbon atom in the $CH_3C^*H(OH)CH_2$– groups introduced by PO. Similar to the ^{1}H-NMR spectra, the ^{13}C-NMR of PEI-PO-NONOates did not exhibit any new resonance peak as compared to PEI-PO. However, the widening and the shifting of the resonance peaks can also be observed due to the changes in the chemical environments.

3.2. NO releasing profiles and stability

As a NO donor, high loading efficiency is one of the most outstanding properties of the PEI-PO-NONOate compound and the evaluation results are shown in Fig. 3. It was found that a

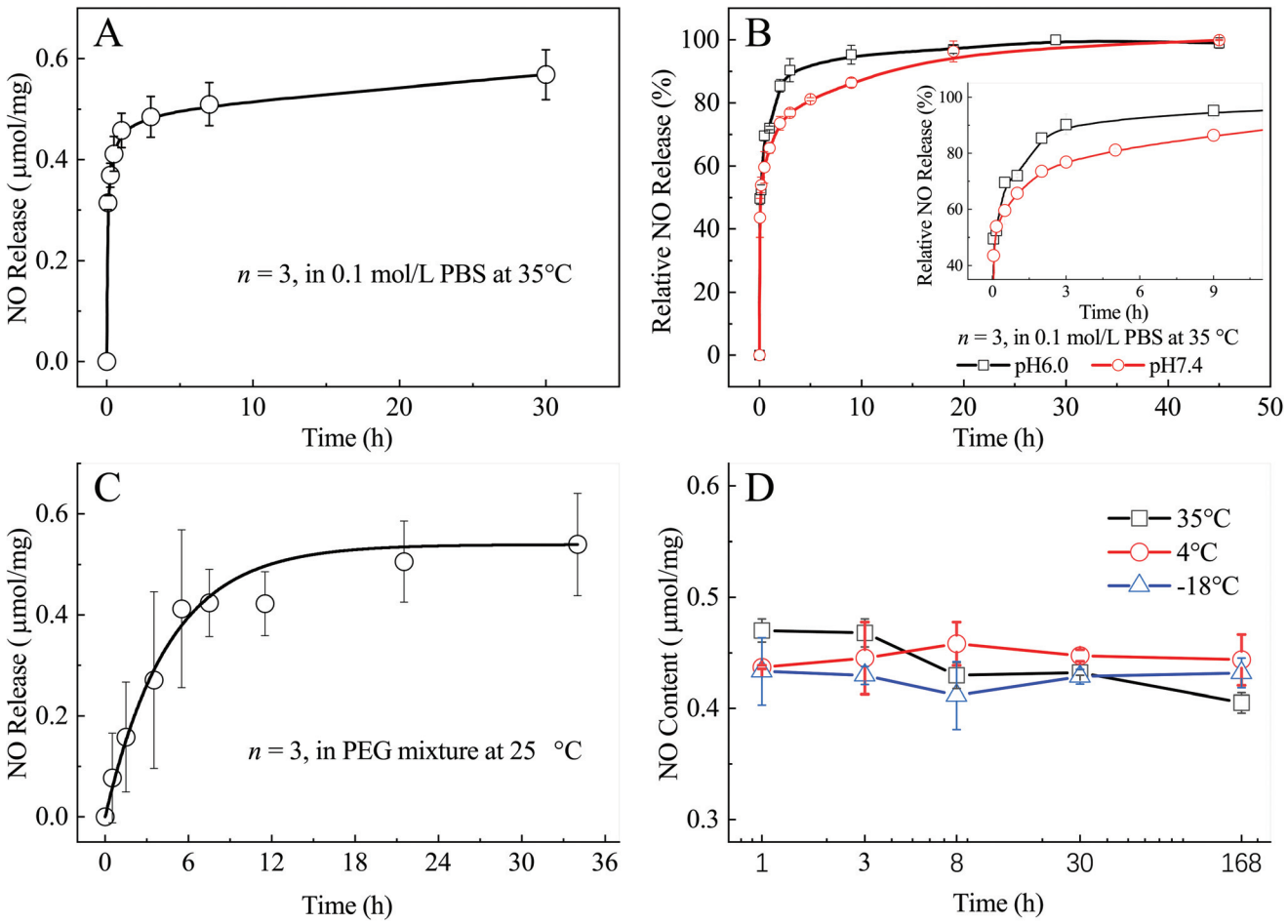

Fig. 3 NO releasing profiles and stability of PEI-PO-NONOates. NO releasing profiles in (A) 0.1 mol L^{-1} PBS of pH7.4 at 35 °C, (B) 0.1 mol L^{-1} PBS of different pH values at 35 °C, and (C) in the PEG mixture system at 25 °C; and (D) stability evaluation of PEI-PO-NONOates under various storage conditions.

total of 0.57 μmol NO was released from 1.0 mg PEI-PO-NONOates (Fig. 3A). Besides, around 65% of NO was released in the first hour when in contact with PBS of pH 7.4 while the remaining NO (35%) was released in the following 29 hours (Fig. 3B). Therefore, the releasing profile can be divided into two stages and a majority of NO was released in the first stage due to the hydrophilicity of the PEI structure and the water-soluble properties of the diazeniumdiolate structure. Under acidic conditions, 72% of NO was released within the first hour because the diazeniumdiolate structure decomposed rapidly in the acidic environment (Fig. 3B), which demonstrated a proton-driven release pattern.

Furthermore, the PEI-PO-NONOate samples were mixed with polyethylene glycol (PEG, MW 400), which is one of the most widely used materials used for making ointments, in order to modulate their consistency for a smooth application on wounds. The NO releasing profile in the PEG mixture system at room temperature was also determined and the results were converted into micro mole per milligram (μmol mg^{-1}) of net PEI-PO-NONOates (Fig. 3C). It displayed a much slower releasing pattern in the PEG mixture as compared to those in PBS. Within the first 12 hours, only about 0.4 μmol NO (70%) was released from 1.0 mg of net PEI-PO-NONOates when the rest of the 30% NO was released gradually in the following 24 hours. The difference obviously stems from the distinct releasing conditions. In PBS, the PEI-PO-NONOate samples dissolved and NO was released fast with the diazeniumdiolate structure decomposing quickly. However, the PEI-PO-NONOate samples did not dissolve in PEG and the decomposition of the diazeniumdiolate structure was much slower, resulting in the slow release of NO. The slow releasing profile of NO in the PEG mixture system is believed to be beneficial for wound healing because of the continuous biological effects as described below.

In order to evaluate the storage stability of the PEI-PO-NONOate compounds, three groups of PEI-PO-NONOate samples were sealed in vials and stored at 35 °C, 4 °C and −18 °C, respectively. It was found that the PEI-PO-NONOate samples remained stable in a cool, dry, and sealed environment for at least 7 days. However, higher ambient temperatures might cause the slow decomposition of

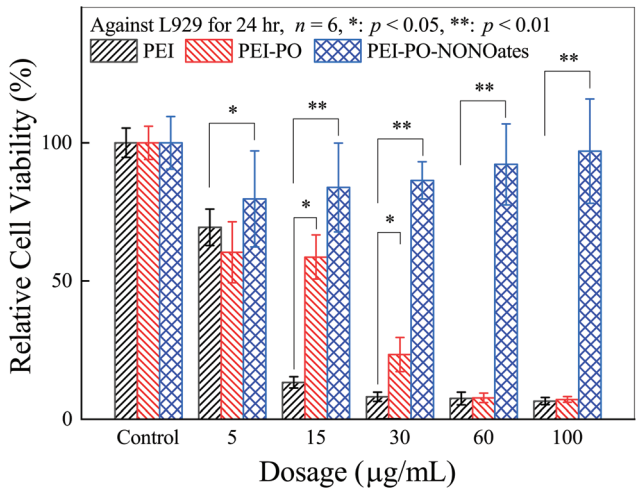

Fig. 4 Cytotoxicity assay of PEI, PEI-PO, and PEI-PO-NONOates against L929 cells, * $p < 0.05$, ** $p < 0.01$.

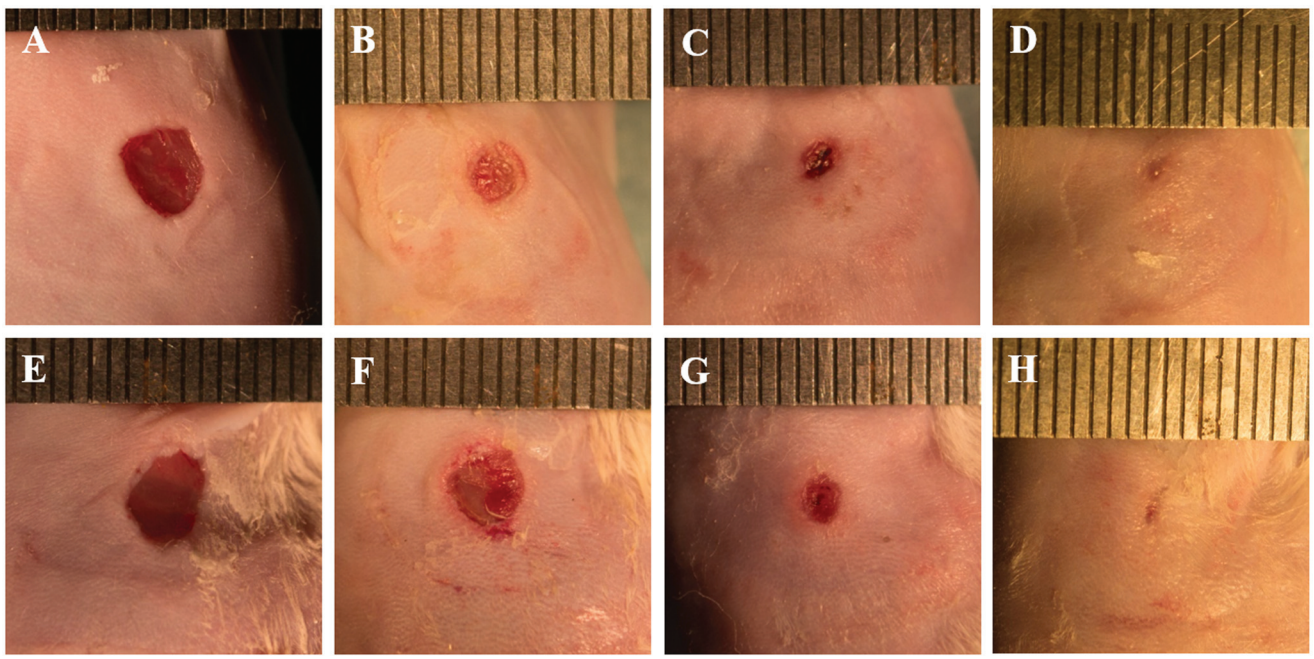

Fig. 5 Nitric oxide accelerated wound healing. Representative images of wounds treated with PEI-PO-NONOates (A) 1, (B) 7, (C) 11, and (D) 14 days post-surgery; and the wounds of the control group (E) 1, (F) 7, (G) 11, and (H) 14 days post-surgery, respectively.

diazeniumdiolates which was reflected in the slight decrease of the residual NO contents of the group stored at 35 °C (Fig. 3D).

3.3. *In vitro* cell cytotoxicity assay

Fig. 4 presents the results of the cytotoxicity assay of PEI, PEI-PO, and PEI-PO-NONOates against L929 cells after incubation for 24 hours. As the dosages ranged from 5 to 100 μg mL^{-1}, PEI showed obvious dosage-dependent cytotoxicity while PEI-PO presented a certain degree of reduction in cytotoxicity. By contrast, PEI-PO-NONOates exhibited no significant cytotoxicity even at a high dosage of 100 μg mL^{-1}. It is known that PEI, particularly with a high molecular weight (*e.g.*, 70 kDa), exhibits cytotoxicity because of the destructive effect of its cationic property on the cell membrane.[23,24] However, PEI with a low molecular weight (*e.g.*, 600 Da) exerts a significantly lower cytotoxic effect.[23,24] Furthermore, after being modified by the addition reaction with PO and NO gas, the cytotoxic effect of PEI-PO-NONOates was substantially reduced which ensured the potential of their application *in vivo*. These results also suggested the cytoprotective effect of NO.

3.4. *In vivo* wound healing assay

The wound areas subjected to NO treatment were 0.167 ± 0.021 cm^2, 0.087 ± 0.024 cm^2, 0.037 ± 0.007 cm^2, and 0.017 ± 0.021 cm^2 on days 1, 7, 11, and 14 post-surgery, whereas those subjected to PEG as the control were 0.172 ± 0.014 cm^2, 0.107 ± 0.015 cm^2, 0.054 ± 0.006 cm^2, and 0.019 ± 0.012 cm^2, respectively (Fig. 5 and 6). The corresponding percentages of wound closure with NO treatment were 48.4 ± 10.5%, 77.1 ± 6.32%, and 88.6 ± 14.1% on days 7, 11, and 14 post-surgery, when those of the control group were 37.2 ± 13.6%, 68.7 ±

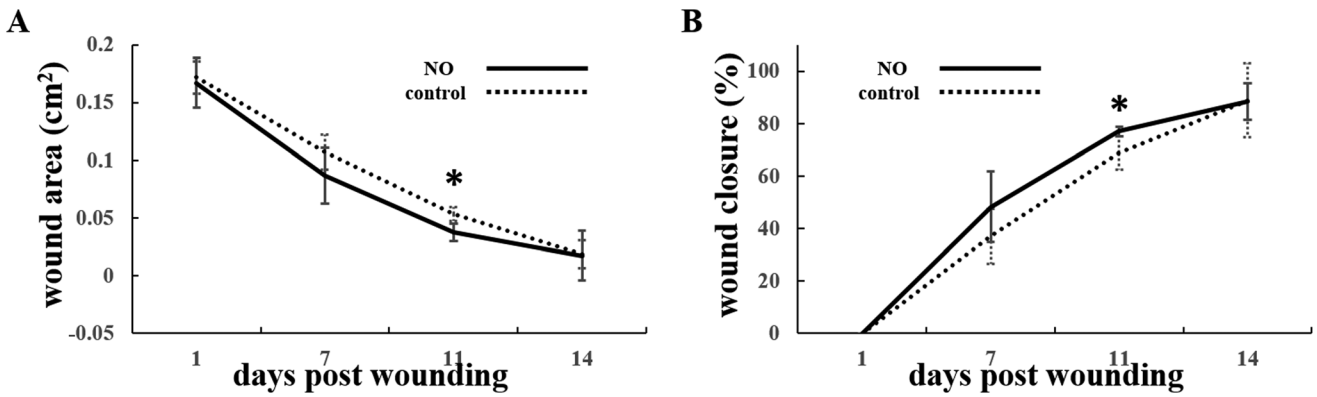

Fig. 6 Nitric oxide promoted wound closure. (A) Wound areas (cm^2) and (B) wound closure (%) of treatment and control groups, * $p < 0.05$.

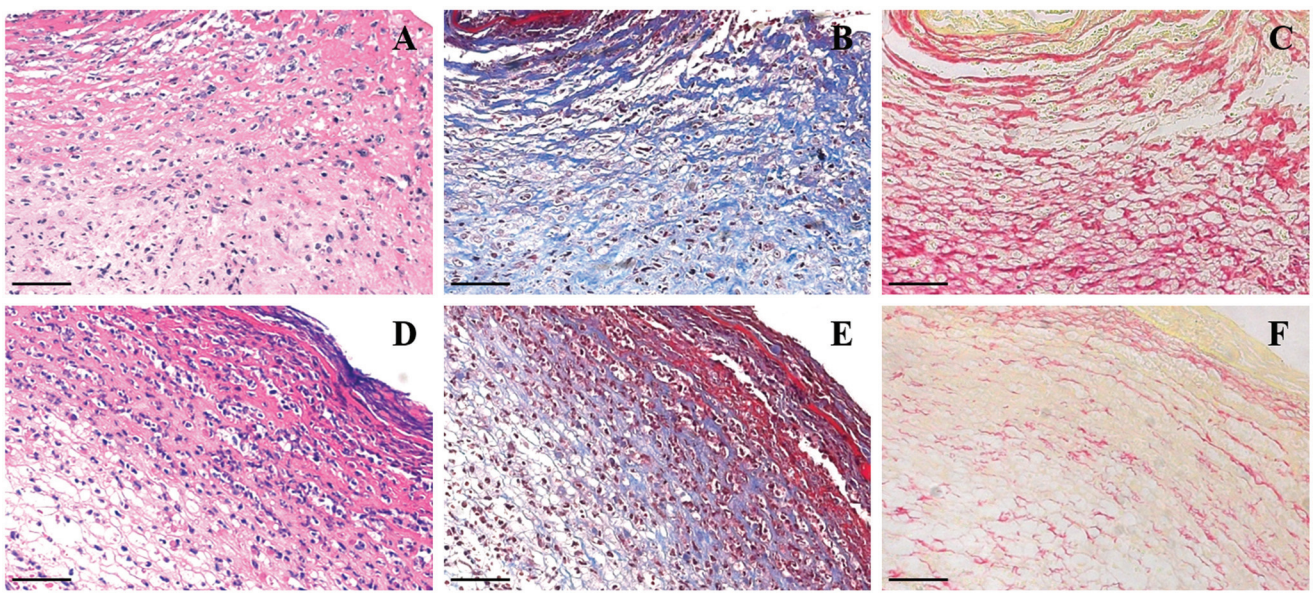

Fig. 7 Nitric oxide promoted granulation tissue formation and collagen deposition. Representative images of (A) HE, (B) Masson trichrome, and (C) Sirius Red staining of wounds treated with PEI-PO-NONOates 7 days after surgery, and images of (D) HE, (E) Masson trichrome, and (F) Sirius Red staining of control wounds 7 days after surgery. Scale bars indicate 50 μm.

1.72%, and 88.9 ± 7.06%, respectively (Fig. 6). These results revealed an apparent tendency that NO treatment accelerated wound repair, although the difference did not achieve statistical significance at some time points. We speculated that these results may be derived from, at least in part, the relatively small wounds created by a punch of 5.0 mm in diameter in view of minimizing the suffering of experimental animals, resulting in a quick recovery trend, overlapping or covering up

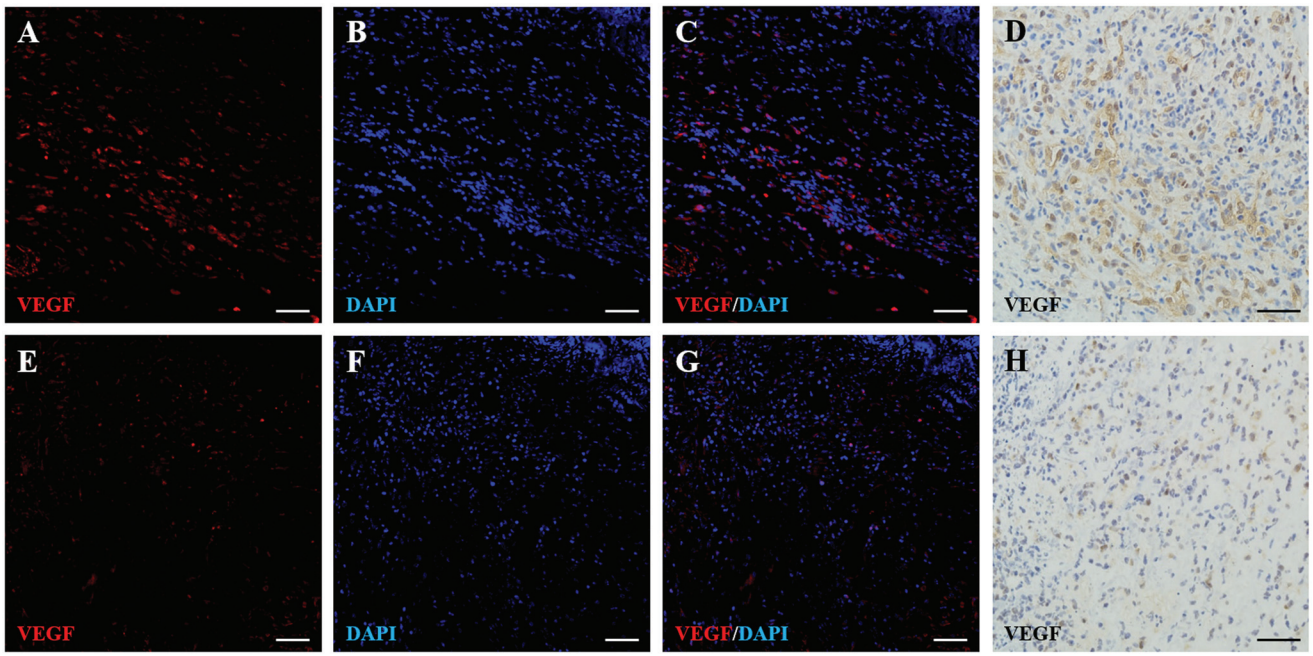

Fig. 8 Nitric oxide promoted VEGF expression. (A) VEGF, (B) DAPI, and (C) merged fluorescence images, and (D) immunohistochemical staining of VEGF of samples treated with PEI-PO-NONOates; (E) VEGF, (F) DAPI, and (G) merged fluorescence images, and (H) immunohistochemical staining of VEGF of samples of the control group. Scale cars indicate 50 μm.

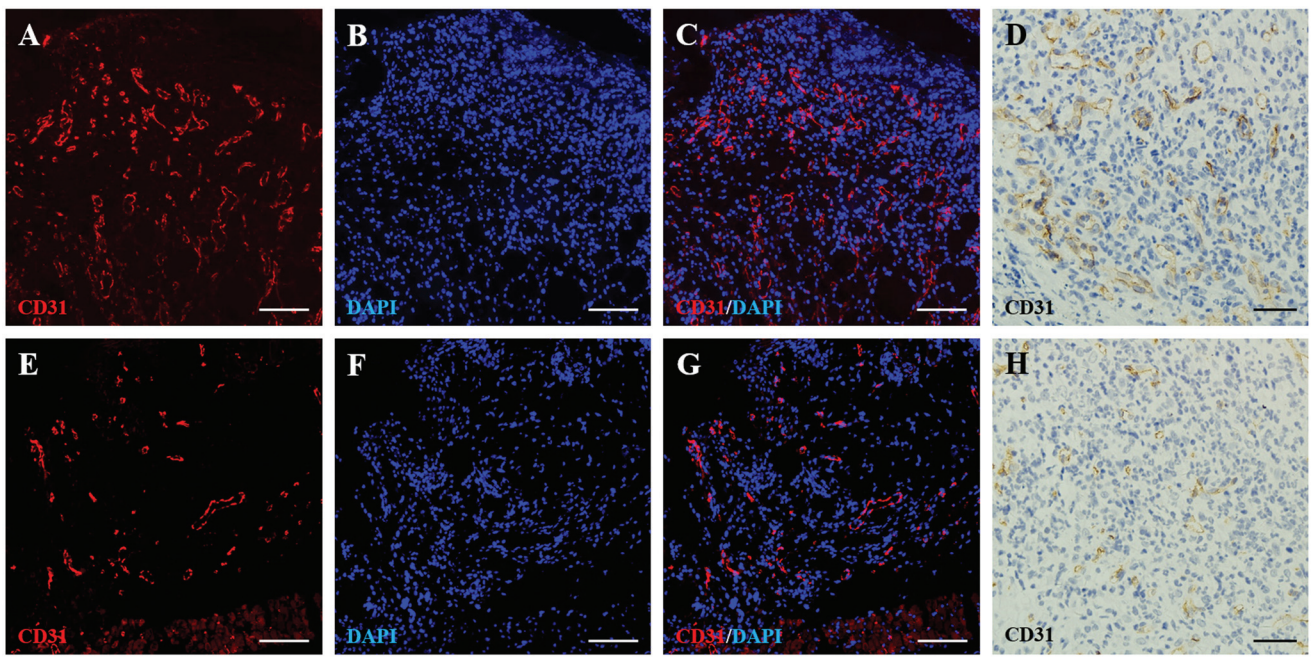

Fig. 9 Nitric oxide promoted angiogenesis as indicated by CD31 expression. (A) CD31, (B) DAPI, and (C) merged fluorescence images, and (D) immunohistochemical staining of CD31 of samples treated with PEI-PO-NONOates; (E) CD31, (F) DAPI, and (G) merged fluorescence images, and (H) immunohistochemical staining of CD31 of samples of the control group. Scale cars indicate 50 μm.

the therapeutic effect to some degree. This phenomenon was also observed in previous studies.[25] Nonetheless, the histopathological experiments further validated and supported the beneficial effects of PEI-PO-NONOates upon wound healing which will be discussed subsequently.

3.5. Histology and immunohistochemistry experiments

Granulation tissue formation, collagen deposition, and angiogenesis are critical processes in wound recovery, which can be promoted by the exogenous supply of NO.[25–28] In this study, hematoxylin–eosin (HE), Masson trichrome and Sirius Red staining were employed to investigate the aforementioned processes. As shown in HE staining images, wounds subjected to PEI-PO-NONOate treatment presented better granulation tissue formation as compared to the control (Fig. 7A and D). Furthermore, Masson trichrome and Sirius Red staining images showed an evident enhanced deposition of collagen in a tight and ordered structure in the wounds treated with PEI-PO-NONOates (Fig. 7B and C). In contrast, collagen deposition in the wounds of the control group exhibited a lower density with a loose arrangement (Fig. 7E and F).

Furthermore, angiogenesis gives rise to the formation of new vessels during wound healing, delivering oxygen and nutrients for tissue repair and reconstruction.[29] The vascular endothelial growth factor (VEGF) is the most important and potent biological stimulator for angiogenesis that maintains the homeostasis of blood vessels, along with extra influences on a variety of mesenchymal stromal cells which are also essential components in the wound repair process.[30,31] Besides, CD31 (also known as platelet/endothelial cell adhesion molecule-1, PECAM-1) which is abundantly expressed in endothelial cells, plays a central role in the maintenance of the vascular integrity and normal functions of vascular endothelial cells.[32,33]

Herein, the pro-angiogenesis effect of PEI-PO-NONOates was investigated by the immunohistochemical and immunofluorescence staining of VEGF as the cytokine which promotes neovascularization and CD31 as the biomarker of vascular endothelial cells.[29,31] As shown in Fig. 8 and 9, the immunohistochemical and fluorescence images indicated an incremental expression level of both VEGF and CD31 in wounds subjected to PEI-PO-NONOates as compared to the control. These results demonstrated the effects of the PEI-PO-NONOate polymer on promoting VEGF expression and subsequent new vessel development.

4. Conclusion

In summary, a novel polyethylenimine based diazeniumdiolate nitric oxide donor (PEI-PO-NONOate) with a high loading efficiency (0.57 μmol NO per 1.0 mg polymer) was designed, prepared and characterized. The PEI-PO-NONOate polymer was stable under anhydrous and sealed conditions with a wide range of temperatures. It presented proton-driven releasing profiles in PBS and displayed a controlled and slow releasing pattern sustaining for over 30 hours in the PEG mixture system. The cytotoxicity analysis indicated that PEI-PO-NONOates exhibited good biocompatibility. The effect of PEI-PO-NONOates on promoting wound healing was investigated on full-thickness excisional cutaneous wound models of mice. The results demonstrated that PEI-PO-NONOates promoted cutaneous wound healing and closure with enhanced granulation tissue formation, collagen deposition, and angiogenesis. Our work demonstrated the great potential of the PEI-PO-NONOate polymer as a nitric oxide donor for the acceleration of cutaneous wound healing. Further investigation is warranted for the determination of the optimal polymer compositions and delivery algorithms.

Conflicts of interest

There are no conflicts of interest to declare.

Acknowledgements

This work is supported in part by the Ph.D. Programs Foundation of Ministry of Education of China (20130171110044), the National Natural Science Foundation of China (81671792), the National Key R&D program of China (2016YFC0104100), the Overseas Study Program of Guangzhou Elite Project (GEP, 11YB18), the Medical Scientific Research Foundation of Guangdong Province of China (A2017025), the Fundamental Research Funds for the Central Universities and the Natural Science Foundation of Guangdong Province of China (2018A030310285). This work is also a part of the Project Funded by the Priority Academic Program Development of Jiangsu Higher Education Institutions (PAPD).

References

1 D. R. Bickers, H. W. Lim, D. Margolis, M. A. Weinstock, C. Goodman, E. Faulkner, C. Gould, E. Gemmen and T. Dall, *J. Am. Acad. Dermatol.*, 2006, **55**, 490–500.
2 H. W. Lim, S. A. B. Collins, J. S. Resneck Jr., J. L. Bolognia, J. A. Hodge, T. A. Rohrer, M. J. Van Beek, D. J. Margolis, A. J. Sober, M. A. Weinstock, D. R. Nerenz, W. Smith Begolka and J. V. Moyano, *J. Am. Acad. Dermatol.*, 2017, **76**, 1151–1160.
3 S. Frank, H. Kampfer, C. Wetzler and J. Pfeilschifter, *Kidney Int.*, 2002, **61**, 882–888.
4 G. I. Broughton, J. E. Janis and C. E. Attinger, *Plast. Reconstr. Surg.*, 2006, **117**, 12s–34s.
5 S. Kumar, R. K. Singh and T. R. Bhardwaj, *Biomed. Pharmacother.*, 2017, **85**, 182–201.
6 S. F. Bernatchez, V. Menon, J. Stoffel, S. A. Walters, W. E. Lindroos, M. C. Crossland, L. G. Shawler, S. P. Crossland and J. V. Boykin Jr., *Wound Repair Regen.*, 2013, **21**, 410–417.

7 A. B. Shekhter, V. A. Serezhenkov, T. G. Rudenko, A. V. Pekshev and A. F. Vanin, *Nitric Oxide*, 2005, **12**, 210–219.
8 G. Badr, W. N. Hozzein, B. M. Badr, A. Al Ghamdi, H. M. Saad Eldien and O. Garraud, *J. Cell. Physiol.*, 2016, **231**, 2159–2171.
9 K. Yamasaki, H. D. Edington, C. McClosky, E. Tzeng, A. Lizonova, I. Kovesdi, D. L. Steed and T. R. Billiar, *J. Clin. Invest.*, 1998, **101**, 967–971.
10 J. Z. Williams, N. Abumrad and A. Barbul, *Ann. Surg.*, 2002, **236**, 369–374.
11 P. C. Lee, A. N. Salyapongse, G. A. Bragdon, L. L. Shears 2nd, S. C. Watkins, H. D. Edington and T. R. Billiar, *Am. J. Physiol.*, 1999, **277**, H1600–H1608.
12 T. P. Amadeu and A. M. Costa, *J. Cutaneous Pathol.*, 2006, **33**, 465–473.
13 C. P. Jenkinson, W. W. Grody and S. D. Cederbaum, *Comp. Biochem. Physiol., Part B: Biochem. Mol. Biol.*, 1996, **114**, 107–132.
14 S. L. Kavalukas, A. R. Uzgare, T. J. Bivalacqua and A. Barbul, *Surgery*, 2012, **151**, 287–295.
15 J. F. Quinn, M. R. Whittaker and T. P. Davis, *J. Controlled Release*, 2015, **205**, 190–205.
16 D. A. Riccio and M. H. Schoenfisch, *Chem. Soc. Rev.*, 2012, **41**, 3731–3741.
17 M. C. Jen, M. C. Serrano, R. van Lith and G. A. Ameer, *Adv. Funct. Mater.*, 2012, **22**, 239–260.
18 A. B. Seabra, G. Z. Justo and P. S. Haddad, *Biotechnol. Adv.*, 2015, **33**, 1370–1379.
19 J. A. Bauer, W. Rao and D. J. Smith, *Wound Repair Regen.*, 1998, **6**, 569–577.
20 J. Kim, Y. Lee, K. Singha, H. W. Kim, J. H. Shin, S. Jo, D. K. Han and W. J. Kim, *Bioconjugate Chem.*, 2011, **22**, 1031–1038.
21 Y. Wo, E. J. Brisbois, R. H. Bartlett and M. E. Meyerhoff, *Biomater. Sci.*, 2016, **4**, 1161–1183.
22 L. K. Keefer, J. L. Flippen-Anderson, C. George, A. P. Shanklin, T. M. Dunams, D. Christodoulou, J. E. Saavedra, E. S. Sagan and D. S. Bohle, *Nitric Oxide*, 2001, **5**, 377–394.
23 C. Brunot, L. Ponsonnet, C. Lagneau, P. Farge, C. Picart and B. Grosgogeat, *Biomaterials*, 2007, **28**, 632–640.
24 Q. Hu, F. Guo, F. Zhao, G. Tang and Z. Fu, *J. Biomater. Sci. Polym. Ed.*, 2017, 28, 768–780.
25 M. Champeau, V. Povoa, L. Militao, F. M. Cabrini, G. F. Picheth, F. Meneau, C. P. Jara, E. P. de Araujo and M. G. de Oliveira, *Acta Biomater.*, 2018, **74**, 312–325.
26 M. B. Witte, F. J. Thornton, D. T. Efron and A. Barbul, *Nitric Oxide*, 2000, **4**, 572–582.
27 G. Han, L. N. Nguyen, C. Macherla, Y. Chi, J. M. Friedman, J. D. Nosanchuk and L. R. Martinez, *Am. J. Pathol.*, 2012, **180**, 1465–1473.
28 Y. Kang, J. Kim, Y. M. Lee, S. Im, H. Park and W. J. Kim, *J. Controlled Release*, 2015, **220**, 624–630.
29 H. Sorg, D. J. Tilkorn, S. Hager, J. Hauser and U. Mirastschijski, *Eur. Surg. Res.*, 2017, **58**, 81–94.
30 K. E. Johnson and T. A. Wilgus, *Adv. Wound Care*, 2014, **3**, 647–661.
31 N. N. Nissen, P. J. Polverini, A. E. Koch, M. V. Volin, R. L. Gamelli and L. A. DiPietro, *Am. J. Pathol.*, 1998, **152**, 1445–1452.
32 J. R. Privratsky, D. K. Newman and P. J. Newman, *Life Sci.*, 2010, **87**, 69–82.
33 J. R. Privratsky and P. J. Newman, *Cell Tissue Res.*, 2014, **355**, 607–619.